

Scaling of Rocket Nozzle Admittances

B. A. Janardan,* B. R. Daniel,* and B. T. Zinn†
Georgia Institute of Technology, Atlanta, Ga.

To apply the admittance data measured experimentally for small-scale nozzles, the necessary scaling criteria must be established. The results of an investigation undertaken to determine these criteria are presented and the data indicate that under cold-flow conditions the damping of axial instabilities provided by full-scale nozzles can be determined from the attenuation data obtained experimentally for geometrically similar small-scale nozzles. The scaling of both short and long nozzles has been investigated. The experimental data also support the scaling criteria proposed by Crocco in his analytical investigation of nozzle damping.

Introduction

THE susceptibility of rocket motors to combustion instability depends upon the wave energy balance between the various gain and loss mechanisms that are present in the system. The primary source of wave energy gain is the combustion process. Energy loss mechanisms are provided by the mean flow, dissipative processes such as viscosity and heat transfer, relaxation processes in the gas phase, nozzle acoustic losses, and the particulate and structural damping. A meaningful stability analysis of a rocket motor would thus involve a quantitative evaluation of all the wave energy gains and losses pertaining to a particular system. A full-scale investigation of the characteristics of the various processes affecting engine stability is a costly and cumbersome, if not an impossible, undertaking. Consequently designers¹⁻⁴ have resorted to the use of small-scale test methods in an effort to obtain quantitative data needed for the determination of engine stability. Notable among these tests are T-burner studies^{5,6} conducted to determine solid propellant response factors and studies conducted to determine rocket nozzle damping.⁷ Although the use of small-scale test data in the determination of engine stability has become a standard practice, there are no known studies in which the validity of this practice has been investigated. In this paper the results of a study undertaken to investigate the scaling criteria that should be employed in using cold-flow, small-scale nozzle damping test data in a stability analysis of a full-scale rocket motor subject to longitudinal instabilities is presented and discussed.

Analytical Scaling Considerations

Nozzle Admittance

To evaluate nozzle damping or wave energy losses in the nozzle, the admittance at the nozzle entrance plane must be determined. The nozzle admittance, Y_N , defined as

$$Y_N = u_1/p_1 \quad (1)$$

is a complex number whose real and imaginary parts describe the relationship that exists at the nozzle entrance between the amplitude and phase of the velocity perturbation u_1 and

Submitted October 16, 1974; presented as Paper 74-1128 at the AIAA/SAE 10th Propulsion Conference, San Diego, California, October 21-23, 1974; revision received January 20, 1975. This research was supported by Air Force Rocket Propulsion Laboratory, Edwards Air Force Base, California, under Contract F04611-71-C-0054. The authors thank W. A. Bell for letting them use the admittance data reported in Ref. 12 for comparison with data generated in the course of this study.

Index categories: Combustion Stability, Ignition, and Detonation; Solid and Hybrid Rocket Engines; Liquid Rocket Engines.

*Research Engineer, School of Aerospace Engineering.

†Regents' Professor of Aerospace Engineering. Associate Fellow AIAA.

pressure perturbation p_1 . These relationships depend upon the wave motion inside the convergent section of the nozzle. The nondimensional form of specific nozzle admittance is written in the following form:

$$Y_N = Y_N/Y_g = \Gamma + i\eta \quad (2)$$

where the reference admittance $Y_g = 1/\bar{\rho}\bar{c}$ is the characteristic admittance of the gas medium at the nozzle entrance.

Considerations of scaling of nozzle admittances give rise to the following two questions: a) what nozzle design features should be reproduced in a small-scale experiment designed to yield meaningful nozzle admittance data; and b) how can nozzle admittance data, measured in cold-flow, small-scale experiments, be used to predict the behavior of full-scale nozzles under normal engine operating conditions? To answer these questions one should determine what variables actually determine the nozzle admittance and then attempt to simulate these variables in a small-scale experiment. To determine these variables, one must consult the analyses that are concerned with the prediction of nozzle admittances.

The theoretical prediction of nozzle admittances is a difficult gas dynamical problem which requires the solution of a mathematically complex system of conservation equations which describe the behavior of the flow oscillations in the convergent section of the nozzle. Available theoretical treatments for computing the nozzle admittance are complex in nature, and, to date, solutions have been obtained only for a limited number of cases. The most sophisticated treatment of the nozzle admittance problem was developed by Crocco and Sirignano,⁸ who considered the case where the wave motion in the nozzle is three-dimensional and the mean flow is one-dimensional. The latter assumption implies a slowly converging nozzle. This theoretical treatment is also applicable to cases where both the wave motion and the steady-state flow are one-dimensional. This theory indicates that for longitudinal mode oscillations the nozzle admittance depends on the nondimensional frequency F (defined as $\omega r_c/\bar{c}$, where \bar{c} is the mean velocity of sound, r_c is the characteristic dimension of the chamber, and ω is the angular frequency), the axial distribution of the steady-state Mach number in the convergent section of the nozzle, and the specific heat ratio. Since the values of the specific heat ratios for different fluids do not differ considerably from each other, Crocco's analysis suggests that, in general, the nondimensional frequency and the mean flow Mach number distribution are the parameters that should be duplicated in the design of small-scale nozzles to be employed in experimental nozzle admittance studies. Crocco's analysis also indicates that the admittance data measured with a reference nozzle having a given entrance Mach number can be used to obtain the admittance data of a "family" of nozzles having the same entrance Mach number and designed by a linear "contraction" or "stretching" of the

reference nozzle. If z_{ref} is the length of the convergent section of the reference nozzle and z_f is the corresponding length of the modified nozzle obtained by "stretching" or "contracting" the reference nozzle, then a scale factor σ can be defined as

$$\sigma = z_f / z_{\text{ref}} \quad (3)$$

Then, according to Crocco's analysis, the nondimensional admittance of the modified nozzle is obtained from the following relationship:

$$[(y_N)_f]_{F=F_f} = [(y_N)_{\text{ref}}]_{F=F_{\text{ref}}} \quad (4)$$

where F_f is given by F_{ref}/σ . The geometrical relationships between the reference and modified nozzles are illustrated in Fig. 1. Examination of this figure indicates that the modified and actual nozzles have similar conical sections but different radii of curvature at the nozzle throat and entrance sections. According to Crocco, the error introduced due to this difference in the shapes of the two nozzles is expected to be negligible.

In separate theoretical investigations, Crocco and Sirignano,⁹ and Zinn¹⁰ have considered the special case where the length of the nozzle convergent section is considerably shorter than the wavelength of the oscillation. According to these references, the nondimensional nozzle admittance y_n can be expressed as follows:

$$y_N = (\bar{\rho}\bar{c}) Y_N = (\gamma - 1) \bar{M}/2 \quad (5)$$

It follows from Eq. (5) that in the case of a short nozzle the specific heat ratio γ and the mean flow Mach number \bar{M} at the nozzle entrance are the only nondimensional parameters that should be reproduced in small-scale experiments designed to measure nozzle admittances. Since variations in the values of γ between different fluids are relatively small, one might expect that perhaps \bar{M} is the only nondimensional parameter that should be reproduced in the small-scale experiments. Intuition and the previously mentioned results of Ref. 8 also suggest that the full-scale and small-scale nozzles should be similar in the sense that the axial distributions of the steady-state Mach numbers in the full-scale nozzles are the same. Adopting the latter criterion results in geometric similarity between the full-scale and small-scale nozzles. Whenever possible, this criterion has been used as a guide in the design of the small-scale nozzles tested in this investigation.

Next, the scaling of cold-flow nozzle admittance data to actual systems will be considered. In applying small-scale nozzle admittance data to actual systems, one needs to verify that the actual nozzle is geometrically similar to the small-scale nozzle. In addition, to obtain data that is applicable to actual systems the cold-flow experiments should be conducted over a range of frequencies whose wavelengths are equal to wavelengths observed during axial instabilities inside the actual engines. The restriction on the wavelength λ , results in the following relationship, when $M^2 \ll 1$:

$$\lambda_H = \lambda_E = 2\pi\bar{c}_H/\omega_H = 2\pi\bar{c}_E/\omega_E \quad (6)$$

where the subscripts H and E represent quantities related to the actual and experimental engines, respectively. Once these criteria have been satisfied, one can obtain the admittance of the actual nozzle from the relationship

$$[Y_N]_H = \frac{\bar{\rho}_E \bar{c}_E}{\bar{\rho}_H \bar{c}_H} [Y_N]_E \quad (7)$$

where $(\bar{\rho}\bar{c}Y_N)_E$ is the experimentally determined admittance, $(Y_N)_H$ is the admittance of the actual nozzle, and $1/\bar{\rho}_H \bar{c}_H$ is the specific admittance of the medium in the "hot" or actual engine.

Nozzle Decay Coefficient

In stability considerations, it is customary to evaluate the effect of the nozzle on the growth/decay rate of a small-amplitude oscillation inside the combustor by evaluating the nozzle decay coefficient α_N . When nozzle is the only factor that can affect the growth or decay of an oscillation inside the combustor, the temporal behavior of the combustor oscillation may be expressed in the following form:

$$p_I(z, t) = P(z) e^{\alpha_N t} e^{i\omega t} \quad (8)$$

The following discussion will outline how the nozzle decay coefficient for an actual engine can be evaluated from the measured cold-flow small-scale nozzle admittance data.

Employing conservation of mass, momentum, and energy considerations, Cantrell and Hart¹¹ arrived at an expression describing the temporal behavior of an acoustic disturbance superimposed upon a mean flow in a rocket combustor. When the nozzle is the only means of wave-energy amplification or attenuation, this temporal growth or decay coefficient can be determined from the following relationship:

$$2\alpha_N \hat{V} = - \int_{\text{nozzle entrance}} dS n \cdot \{ p_I u_I + (\bar{M}/\bar{\rho}\bar{c}) p_I^2 + \bar{\rho}\bar{c}(\bar{M} \cdot u_I) u_I + (\bar{M} \cdot u_I) p_I \bar{M} \} > \quad (9)$$

where

$$\hat{V} = \int_{\text{combustor volume}} dV \{ \frac{1}{2} \bar{\rho} u_I \cdot u_I + \frac{1}{2} (p_I^2 / \bar{\rho}\bar{c}^2) + (\bar{u} \cdot u_I / \bar{c}^2) p_I \} > \quad (10)$$

and n is a unit normal vector pointing out of the combustor. The time average $< >$ is defined as

$$< > = \lim_{T \rightarrow \infty} \frac{1}{T} \int_0^T () dt$$

An examination of Eqs. (9) and (10) indicates that the acoustic mode structure and the mean flow properties inside the combustor must be known to evaluate α_N . Assuming one-dimensional uniform flow at the nozzle entrance plane Eq. (9), can be reduced to the following form:

$$\left(\frac{2\bar{\rho}\bar{c}\hat{V}}{S_N |P_N|^2} \right) \alpha_N = - \{ (1 + \bar{M}^2) Re\{y_N\} + \bar{M} + \bar{M} |y_N|^2 \} \quad (11)$$

where $|P_N|$ is the pressure amplitude at the nozzle entrance. Both sides of Eq. (11) are nondimensional, and the quantity on the left-hand side may be considered as a parameter describing the acoustics of the combustor while the expression on the right-hand side of this equation may be considered as describing the acoustic properties of the nozzle. Three of the four terms that appear on the right-hand side of this equation depend upon the steady flow Mach number at the nozzle entrance plane, and they can be considered as representing wave energy losses due to the presence of a mean flow. The remaining term can be considered as representing the radiative wave energy loss out of the nozzle.

Suppose two nozzles having the same admittance y_N and the same mean flow Mach number \bar{M} at their entrances are attached to two different combustors, and suppose one would like to determine the nozzle decay coefficient of one of these combustors by investigating the behavior of the other combustor, which in this discussion will be taken to be the cold flow, small-scale chamber used in the present study. Equation (11) can be applied to both systems in order to determine their α_N . However, since the nozzles of both systems are assumed

to be geometrically similar, then the right-hand side of Eq. (11) will be the same for both engines, and one can write

$$\left(\frac{\bar{\rho} \bar{c} \alpha_N \hat{V}}{S_N |P_N|^2} \right)_H = \left(\frac{\bar{\rho} \bar{c} \alpha_N \hat{V}}{S_N |P_N|^2} \right)_E$$

$$= -\frac{1}{2} [(I + \bar{M}^2) \operatorname{Re}\{y_N\} + \bar{M} + \bar{M} |y_N|^2]_E \quad (12)$$

Rearranging Eq. (12) yields

$$(\alpha_N)_H = \frac{\bar{\rho}_E \bar{c}_E}{\bar{\rho}_H \bar{c}_H} \frac{(S_N)_H}{(S_N)_E} \frac{\{\hat{V}/|P_N|^2\}_E}{\{\hat{V}/|P_N|^2\}_H} (\alpha_N)_E \quad (13)$$

Examination of Eq. (13) shows that the scaling of the nozzle decay coefficient data depends upon knowledge of the specific acoustic impedances $\bar{\rho} \bar{c}$ of both media at the nozzle entrance planes, knowledge of nozzle entrance areas S_N , and knowledge of the structures of the acoustic modes inside the combustors as represented by the parameter $\hat{V}/|P_N|^2$. Determination of the specific acoustic impedance of the media requires knowledge of the actual temperature and composition of the gases at the nozzle entrance, and the determination of the parameter $\hat{V}/|P_N|^2$ requires knowledge of the acoustic mode structure inside the combustor. While the parameter $\hat{V}/|P_N|^2$ can be easily determined for relatively simple acoustic systems, its determination for complex geometries with mean flows found in actual rockets, is a formidable if not an impossible task.

Before ending this section, it should be pointed out that the formulas for the determination of α_N are based on knowledge of the nondimensional nozzle admittance y_N . However, nozzle admittance data are usually obtained in experiments where amplitude of chamber oscillation neither grows nor decays with time. Hence, when one uses such an admittance to compute the nozzle decay coefficient, one is implicitly assuming that the available nozzle admittance, which was measured under conditions of constant wave amplitude, is also applicable to situations in which the amplitude of the oscillation changes with time.

Admittance Measurements

Experimental Technique

In the present investigation, the nozzle admittances were measured using the modified impedance-tube technique. In this method, a sound source capable of generating simple harmonic waves of desired frequencies and wave forms is placed at one end of a simulated rocket chamber or a modified impedance tube. The test nozzle is attached to the other end of the chamber. Due to the convergence of the nozzle walls and the presence of mean flow gradients in the convergent section of the nozzle, an incident axial wave generated by the acoustic driver, is partially reflected at the nozzle entrance plane. The reflected wave interacts with the incident wave to form a standing wave pattern in the simulated rocket combustor. The nozzle admittance is determined by measuring the axial variations of the pressure wave amplitude and phase along the modified impedance tube. The time and spatial dependence of the pressure perturbation can be expressed in the following form:^{12,13}

$$p_I(z, t) = P_I(z) e^{i(\delta + \omega t)} \quad (14)$$

where the pressure amplitude $P_I(z)$ is given by

$$P_I(z) = A \left[\cosh^2(\pi \alpha) - \cos^2 \pi \left\{ \left(\beta + \frac{(\omega/\bar{c})}{\pi(I - \bar{M}^2)} z \right) \right\} \right]^{1/2} \quad (15)$$

and pressure phase $\delta(z)$ is given by

$$\delta(z) = \frac{(\omega/\bar{c})}{(I - \bar{M}^2)} z + \operatorname{Arctan} [\tanh(\pi \alpha) / \tan \pi \beta] + \frac{(\omega/\bar{c})}{\pi(I - \bar{M}^2)} z \quad (16)$$

The two admittance parameters α and β appearing in Eqs. (15) and (16), respectively, describe the changes in amplitude and phase between the incident and reflected pressure waves at the nozzle entrance;¹⁴ that is

$$\left[\frac{\text{Amplitude of reflected pressure wave}}{\text{Amplitude of incident pressure wave}} \right]_{\text{nozzle entrance}} = e^{-2\pi \alpha} \quad (17)$$

$$\left[\frac{\text{Phase change between incident and reflected pressure waves}}{\text{nozzle entrance}} \right] = \pi(I + 2\beta) \quad (18)$$

where the parameter β must satisfy the restriction $|\beta| \leq 0.5$. An examination of Eqs. (17) and (18) indicates that the unknowns α , β , and A can be determined by measuring the pressure amplitudes and/or phases at three different locations along the chamber. The resulting values of the admittance parameters α and β are then substituted into the following equation^{12,13}

$$y_n = \Gamma + i\eta = \coth \pi(\alpha - i\beta) \quad (19)$$

to obtain the nozzle admittance.

Experimental Apparatus

In this investigation, admittances of geometrically similar small- and large-scale nozzles were measured using two impedance tubes with inside diameters of 11-3/8 and 7-5/8 in. respectively. Along the length of each of these tubes, ports are provided for the installation of acoustic drivers, dynamic pressure transducers, thermocouples, and static pressure orifices. To improve the accuracy of the measured admittance data, ten pressure transducers, placed at different locations along the length of the tube, were used in the present investigation. During a test, the driver frequency was varied continuously over the range of 40-600 Hz at the rate of 8 Hz/sec. Analog pressure and temperature data recorded on a tape recorder during each test were later digitized and analyzed by use of a Fourier analysis to determine the amplitudes and phases of the chamber pressure oscillations as a function of the driver frequency. The unknown admittance parameters were then computed by use of a nonlinear regression analysis that provides the best fit between the amplitude and phase data and the corresponding amplitude and phase expressions as given by Eqs. (15) and (16). Detailed description of the experimental technique and the apparatus is given in Refs. 12 and 13.

Test Nozzles

The validity of the previously discussed scaling criteria has been investigated by measuring the admittances of two sets of geometrically similar rocket nozzles. Each set of nozzles consisted of: a) a short single-ported solid rocket nozzle; b) a short multiple-ported solid rocket nozzle; and c) a conical liquid rocket nozzle. The set of larger nozzles were assumed to represent the "full-scale" nozzles and their admittances were measured using the 11-3/8 in. impedance tube while the set of

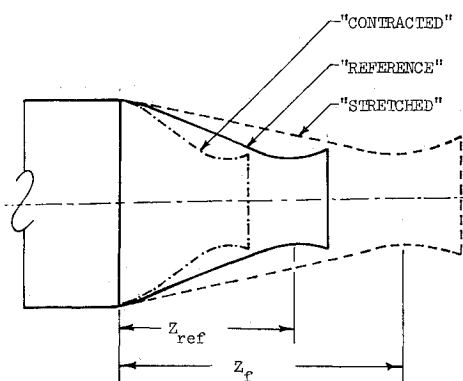


Fig. 1 "Family" of scaled nozzles.

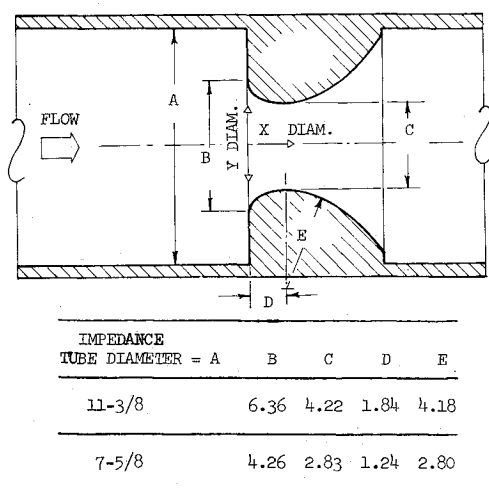


Fig. 2 Single-ported solid rocket nozzle. (All dimensions in inches.)

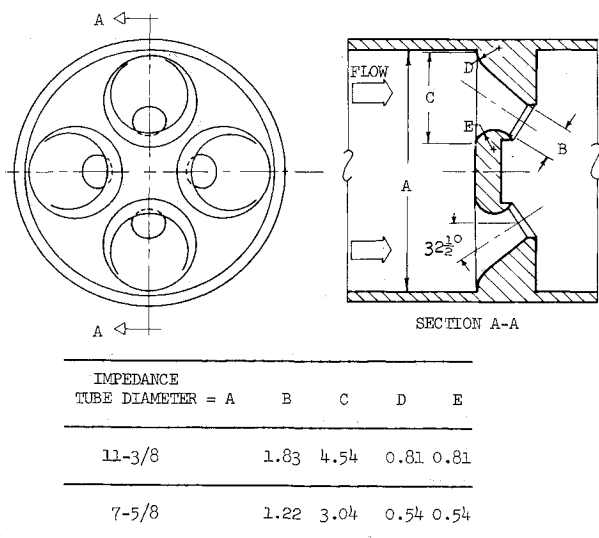


Fig. 3 Multiple-ported solid rocket nozzle. (All dimensions in inches.)

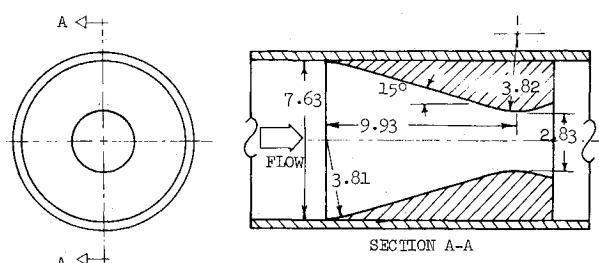


Fig. 4 15° conical liquid rocket nozzle. (All dimensions in inches.)

smaller nozzles represented the "small-scale" geometrically similar nozzles and their admittances were measured using the 7-5/8 in. impedance tube. The nozzle configurations tested in this study are shown in Figs. 2-4.

Results

The results presented in this section were obtained by investigating the acoustic responses of geometrically similar nozzles, under cold-flow conditions, over a range of frequencies whose wavelengths are equal to the wavelengths observed during axial instabilities inside typical solid propellant rocket motors. The repeatability of the measured data is demonstrated in Ref. 15. This reference also contains a discussion on uncertainties associated with the measured data.

The measured admittance data of the short nozzles were found to be practically independent of the frequency. The measured data is summarized in Table 1 along with data predicted by the short nozzle theories discussed in Refs. 9 and 10. The experimental nondimensional nozzle decay coefficient, Λ_N (defined as equal to $\alpha_N L_c / \bar{c}$, where L_c is the length of the simulated combustor), was calculated from the measured admittance data using Eq. (11). This calculation is discussed in detail in Ref. 13. A comparison of the admittance data obtained with the "full-scale" nozzles, tested in the 11-3/8 in. impedance tube, with the corresponding data obtained with the "small-scale" nozzles, tested in the 7-5/8 in. impedance tube, shows a good agreement between the two sets of data. This good agreement supports the assertion that damping of axial instabilities by short nozzles can be determined by measuring the admittances of geometrically similar small-scale nozzles.

A comparison of the measured admittance data with the corresponding theoretical predictions indicates that the test nozzles behave as short nozzles in the sense that their admittances are independent of the frequency. However, the experimentally measured values of the real and imaginary parts of the nondimensional admittance and decay coefficient are larger than the corresponding theoretical predictions. This discrepancy is believed to be due to the presence of entropy waves which are not taken into account in the theoretical treatment of this problem.

The scaling of the admittance data of the nozzle shown in Fig. 4 is more complex than the scaling of the admittance data of short nozzles because of the difference in the lengths of their convergent sections. It has been shown in Ref. 12 that the magnitudes and frequency dependence of the admittances

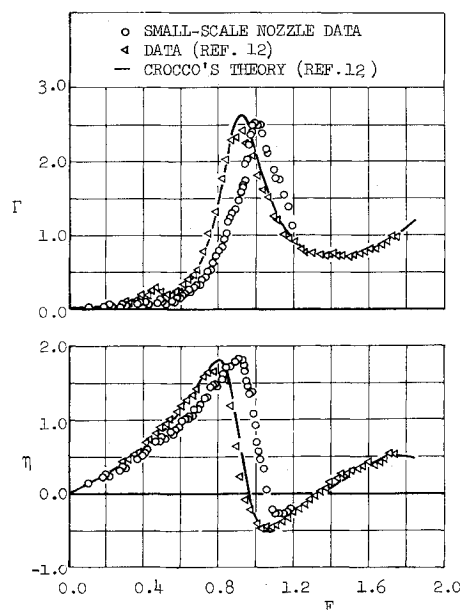


Fig. 5 Admittance data of the 15° conical nozzle.

Table 1 Summary of the single-ported and multiple-ported nozzle admittance data

Nozzle	Impedance tube diameter (in.)	Chamber Mach number	Experimental data					Theoretical data based on Refs. 9 and 10		
			α	β	Γ	η	Λ_N	Γ	η	Λ_N
Single ported	11-3/8	0.08	0.014	± 0.495	0.044	± 0.016	-0.123	0.016	0.00	-0.096
	7-5/8	0.08	0.015	± 0.495	0.047	± 0.016	-0.126			
Multiple ported	11-3/8	0.06	0.012	0.480	0.038	0.063	-0.097	0.012	0.00	-0.072
	7-5/8	0.06	0.010	0.485	0.032	0.047	-0.091			

of the conical nozzle shown in Fig. 4 are entirely different from the magnitudes and frequency dependence of the admittances of the other two nozzle configurations tested in this study. The "full-scale" conical nozzle admittance data were obtained¹² by testing the larger nozzle in the 11-3/8 in. impedance tube while the "small-scale" nozzle admittance data for this configuration were obtained by measuring the admittances of a small-scale geometrically similar nozzle in the 7-5/8 in. impedance tube. A comparison of the two sets of admittance data is presented in Fig. 5. Examination of Fig. 5 indicates that while the two sets of data are similar in magnitudes and shapes, there is a slight frequency between them. For example, the maximum value of Γ obtained during the present investigation occurs at $F=0.99$ while the corresponding peak in the data presented in Ref. 12 occurs at $F=0.91$, indicating a frequency shift of 0.08.

When various efforts to explain the observed frequency shift did not produce any significant results, the dimensions of the small-scale nozzle were checked to ensure that it had been machined according to specifications. This examination showed that the length of the convergent section of the tested small-scale nozzle measured 9.13 in. instead of the design length of 9.93 in. and the half-angle of the nozzle convergent section measured 16.75° instead of the design angle 15° . It will now be shown that this discrepancy in the actual nozzle length is the cause of the observed frequency shift in the measured admittance data.

Earlier in this paper, Crocco's analysis was used to show how the admittance data of a reference nozzle can be employed to determine the admittances of a "family" of nozzles obtained by a linear "contraction" or "stretching" of the reference nozzle. It follows from this discussion that the admittances $(y_N)_f$ of the nozzle illustrated in Fig. 4 ($z_f=9.93$ in.) can be obtained from the measured admittances $(y_N)_{ref}$ by considering the nozzle of Fig. 4 as a "stretched" version of the tested nozzle ($z_{ref}=9.13$ in.). Using Eq. (3) and the lengths of the reference and "stretched" nozzles, it can be shown that the scale factor σ that is associated with the "stretched" nozzle equals 1.09. Using Eq. (4) the admittance data of the scaled nozzle illustrated in Fig. 4 is given by

$$[(y_N)_f]_{F=F_f} = [(y_N)_{ref}]_{F=F_{ref}} \quad (4)$$

where

$$F_f = F_{ref}/\sigma \quad (19)$$

To illustrate the use of these equations the frequency at which the real part of nondimensional admittance of the "stretched" nozzle is a maximum will be calculated. It is shown in Fig. 5 that the corresponding maximum for the "reference" nozzle occurs at $F_{ref}=0.99$. Using the scale factor the maximum value in Γ for the "stretched" nozzle occurs at $F_f=0.99/1.09=0.91$. As mentioned earlier in this discussion this was the frequency at which the maximum value in Γ was observed in Ref. 12. Equation (19) can be rewritten as

$$F_{ref} - F_f = [(\sigma - 1)/\sigma] F_{ref} \quad (20)$$

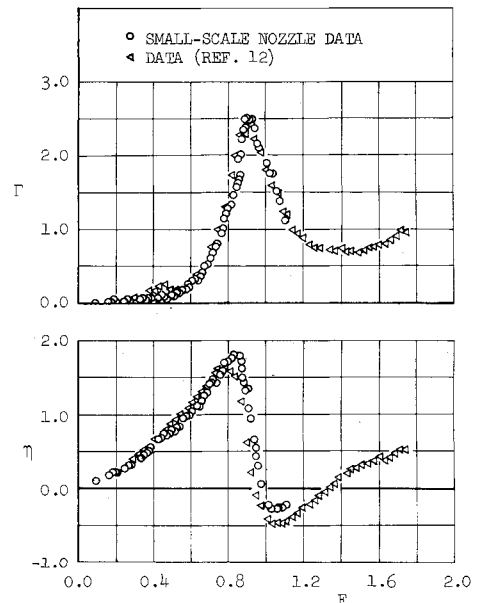


Fig. 6 Comparison of small-scale conical nozzle admittance data.

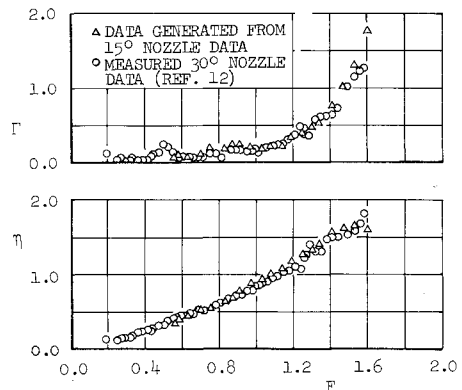


Fig. 7 Comparison of 30° nozzle admittances with data predicted from admittances of 15° "reference" nozzle.

With $\sigma=1.09$, Eq. (20) reduces to $(F_{ref}-F_f)=0.0825F_{ref}$. This is the frequency shift that needs to be applied to the measured admittance data in order to generate the admittance data of the "stretched" nozzle. Applying this frequency correction to the measured data presented in Fig. 5, the admittance data of the "stretched" nozzle were obtained and are presented in Fig. 6. An examination of this figure indicates that the admittance data of the "stretched" nozzle are in good agreement with the corresponding data of Ref. 12. As mentioned earlier, the "stretched" nozzle is the one which is geometrically similar to the nozzle tested in Ref. 12.

The long nozzle data support Crocco's⁸ suggestion that the admittances of a "family" of nozzles having the same entrance Mach number can be obtained from the admittance

data of a reference nozzle. Additional experimental verification of this useful conclusion was obtained by generating additional data using the experimental data reported in Ref. 12. This reference contains, in addition to the admittance data plotted in Fig. 5 for the 15° conical nozzle, measured admittance data of a 30° conical nozzle. The admittance data for both these nozzles were measured, with an entrance Mach number of 0.08, using the 11-3/8 in. modified impedance tube. Hence, these two nozzles can be considered as belonging to the same "family" of nozzles. Considering the 15° conical nozzle ($z_{\text{ref}} = 14.85$ in.) as the reference nozzle, its measured admittances together with Eqs. (4) and (19) have been used to predict the admittances of the 30° conical nozzle ($z_f = 7.5$ in.). The generated admittance data were then compared with the measured admittance data for the 30° conical nozzle reported in Ref. 12. These two sets of data are plotted in Fig. 7. The good agreement indicated in this figure provides additional support to the validity of Crocco's conclusion.

Conclusions

The data obtained in this study support Crocco's⁸ conclusion that the admittances of a reference nozzle with a given entrance Mach number can be used to obtain the admittances of a "family" of nozzles having same entrance Mach number and designed by a linear "contraction" or "stretching" of the reference nozzle. In addition, the measured admittance data indicate that damping of axial instabilities by full-scale nozzles can be investigated by experimentally determining the behavior of geometrically similar small-scale nozzles. It remains, however, to prove that the nozzle admittance data measured under cold flow conditions are also applicable to real engine operating conditions where the gases are considerably hotter than the air used for testing in this program. Investigation of this point would require the repetition of this study at elevated temperatures. The high-temperature experiments were not attempted during the present investigation.

References

- ¹Hart, R. W. and Bird, J. F., "Scaling Problems Associated with Unstable Burning in Solid Propellant Rockets," *Ninth Symposium (International) on Combustion*, The Combustion Institute, Pittsburgh, Pa., 1962, pp. 993-1004.
- ²Lawhead, R. B. and Combs, L. P., "Modeling Techniques for Liquid Propellant Rocket Combustion Processes," *Ninth Symposium (International) on Combustion*, The Combustion Institute, Pittsburgh, Pa., 1962, pp. 973-981.
- ³Crocco, L., "Considerations of the Problem of Scaling Rocket Motors," *Selected Combustion Problems*, II, Butterworth, London, 1956.
- ⁴Panel Discussion, *Eighth Symposium (International) on Combustion*, The Combustion Institute, Pittsburgh, Pa., 1962, pp. 904-932.
- ⁵Price, E. W., "Experimental Solid Rocket Combustion Instability," *Tenth Symposium (International) on Combustion*, The Combustion Institute, Pittsburgh, Pa., 1965, pp. 1067-1082.
- ⁶Coates, R. L. and Horton, M. D., "Design Considerations for Combustion Instability," *Journal of Spacecraft and Rockets*, Vol. 6, March 1969, pp. 296-302.
- ⁷Buffum, F. G., Dehority, G. L., Slates, R. O., and Price, E. W., "Acoustic Attenuation Experiments on Subscale Cold-Flow Rocket Motors," *AIAA Journal*, Vol. 5, Feb. 1967, pp. 272-280.
- ⁸Crocco, L. and Sirignano, W. A., *Behavior of Supercritical Nozzles Under Three-Dimensional Oscillatory Conditions*, ADGARDograph 117, 1967, Princeton University, Princeton, N.J.
- ⁹Crocco, L. and Sirignano, W. A., "Effect of Transverse Velocity Components on the Nonlinear Behavior of Short Nozzles," *AIAA Journal*, Vol. 4, Aug. 1966, pp. 1428-1430.
- ¹⁰Zinn, B. T., "Longitudinal Mode Acoustic Losses in Short Nozzles," *Journal of Sound and Vibration*, Vol. 22, May 1972, pp. 93-105.
- ¹¹Cantrell, R. A. and Hart, R. W., "Interaction Between Sound and Flow in Acoustic Cavities; Mass, Momentum and Energy Considerations," *Journal of the Acoustical Society of America*, Vol. 36, April 1964, pp. 697-706.
- ¹²Bell, W. A., Daniel, B. R., and Zinn, B. T., "Experimental and Theoretical Determination of Admittances of a Family of Nozzles Subjected to Axial Instabilities," *Journal of Sound and Vibration*, Vol. 30, Sept. 1973, pp. 179-190.
- ¹³Janardan, B. A., "Damping of Axial Instabilities by Solid Propellant Rocket Exhaust Nozzles," Ph.D. thesis, Aug. 1973, School of Aerospace Engineering, Georgia Institute of Technology, Atlanta, Ga.
- ¹⁴Morse, P. M. and Ingard, K. V., *Theoretical Acoustics*, McGraw-Hill, New York, 1968.
- ¹⁵Janardan, B. A., Daniel, B. R., and Zinn, B. T., "Damping of Axial Instabilities by Small-Scale Nozzles under Cold-Flow Conditions," *Journal of Spacecraft and Rockets*, Vol. 11, Dec. 1974, pp. 872-820.